Supporting Information

Louis et al. 10.1073/pnas.1709037115

SI Materials and Methods

Fly Strains. Flies were maintained on cornmeal/agar food, with 12:12-h light:dark cycles, using standard *Drosophila* laboratory protocols. MB-specific Gal4 drivers were selected to include drivers in widespread previous use (238Y, c739, c305, and 1471), Gal4 drivers from the Janelia collection (R13F02, R64C08, R35B12, and R34B09), and split-Gal4 driver combinations from the Janelia collection (MB009B, MB005B, MB008B, and MB461B). Female flies aged 2 to 10 d were used in all imaging experiments, except CaMPARI (as noted below). Mixed populations of males and females were used for behavior.

Fly Preparation for in Vivo Ca^{2+} Imaging. Flies were briefly anesthetized, placed in a polycarbonate imaging chamber, and fixed with myristic acid (Sigma-Aldrich). The proboscis was fixed in the retracted position, except for appetitive conditioning experiments (as noted below). A cuticle window was opened, and the fat and tracheal air sacs were carefully removed to allow optical access to the brain. The top of the chamber was filled with saline solution (103 mM NaCl, 3 nM KCl, 5 mM Hepes, 1.5 mM $CaCl_2$, 4 mM $MgCl_2{\cdot}6H_2O$, 26 mM $NaHCO_3$, 1 mM $NaH_2PO_4{\cdot}H_2O$, 10 mM trehalose, 7 mM sucrose, and 10 mM glucose), which was perfused over the dorsal head/brain at 2 mL/min via a peristaltic pump.

In Vivo Ca^{2+} Imaging. Several GCaMP variants—cytosolic GCaMP6f, presynaptically tethered syp-GCaMP3, or postsynaptically tethered homer-GCaMP3—were expressed in projection neurons or MB γ-, α/β-, and/or α′/β′-neurons with various Gal4 or split-Gal4 drivers. These include the projection neuron driver GH146, broad MB drivers 238Y and R13F02, MB γ-selective 1471, R64C08, and MB009B, MB α/β-selective c739, R34B09, and MB008B, and MB α′/β′-selective c305, MB461B, and MB005B (1, 2). The β-, γ1-, and γ2–5-regions were imaged in separate regions of interest (ROIs) within one plane of section, except where noted. The α-lobe was imaged in the tip (α3) region for most experiments (3). However, the upper stalk (α2) was imaged in aversive conditioning experiments to capture the presynaptic activity in the compartment where an aversive MB output neuron memory trace was reported (4). Ca^{2+} reporters were imaged with confocal microscopy by using appropriate laser lines and emission filter settings on a Leica TCS SP8 confocal microscope. Odors were presented by redirecting an airstream (60 mL/min flow rate) from an empty vial to one containing 1 μL odorant on filter paper via solenoid valves. Responses were plotted as the baseline-normalized change in GCaMP fluorescence ($\Delta F/F$). The post/pre response was calculated as the ratio of the post- and pretreatment maximum $\Delta F/F$ within the 8 s following odor onset.

Single-Cell Imaging. Flies were prepared for imaging as above, except that muscle M16 was cut to reduce brain movement. GCaMP6f was expressed in subsets of MB neurons using different Gal4 drivers. A single *z* plane was imaged and individual ROIs were drawn around well-separated individual somata. Odor-evoked responses were recorded pre- and posttreatment, and only neurons that exhibited a response in at least one of these times were included in the analysis. Responses of individual neurons were categorized (increased, decreased, or no change) by comparison of the time series traces before and after treatment. The 8-s time segment encompassing the odor-evoked Ca^{2+} response (15 to 23 s into the recording) was analyzed, comparing pre- and posttreatment values with a Wilcoxon rank-sum test. If a difference was detected at the α 0.05 level, the response was classified as having significantly changed and categorized as an increase or decrease.

Pharmacological and Optogenetic Manipulation of cAMP in Vivo. Forskolin was used to elevate cAMP as previously described (5). MB responses were imaged from flies expressing either GCaMP6f or UAS-epac-camps in the MB (5, 6). Forskolin or the control drug 1,9-dideoxyforskolin was perfused with a peristaltic pump into the recording chamber for 30 s, and washed out for 5 min. GCaMP responses were imaged before and after cAMP manipulations, and cAMP responses were imaged during application and washout. For optogenetic elevation of cAMP, R-GECO (7) and bPAC (8) were coexpressed in MB neurons using the 238Y-Gal4 driver. To activate bPAC, the brain was illuminated with blue laser light (448 nm) for 1 min at 10 Hz (paired with a 30-s odor presentation). Odor-evoked Ca^{2+} responses were imaged before and after the pairing, as described above, and the ratio between the post- and pretreatment response peaks was calculated for each fly. Imaging of odor-evoked transients with R-GECO and optogenetic elevation of cAMP were temporally separated, avoiding any artifactual activation of R-GECO with blue light (9).

Activity-Dependent Neuronal Tagging in Vivo. Flies expressing the high-affinity CaMPARI reporter (10) under the control of either a γ-specific (1471-Gal4) or α/β-specific (c739-Gal4) driver were imaged 10 to 20 d posteclosion. Odor was presented to the flies (10× 1-s pulses), and then paired with forskolin or saline (controls) for 30 s. The subset of neurons responsive to the odor was subsequently tagged by pairing odor presentation with 405-nm UV light through a cuticle window via a fiber-coupled LED (Thorlabs). To optimize the photoconversion of the CaMPARI protein, the flies received 10× 1-s odor pulses, each of which was paired with 5× 500-ms UV light stimulation with 200-ms interpulse interval (2.5 s total). The UV pulses were empirically adjusted to overlap with the ∼2.5-s Ca^{2+} response evoked by odor stimulation. The interval between the onset of each of the 10 odor pulses was 30 s. After the pairing, the saline solution was replaced with Ca^{2+}-free saline (10). A *z* stack encompassing the complete region of the MB somata was collected for both the green and red channels. Images were processed in Fiji (11) and the number of photoconverted cells was counted.

Aversive Conditioning. Flies were prepared for in vivo imaging and trained with a modified aversive classical conditioning paradigm under the microscope (12–14). The odorants used for all conditioning experiments were ethyl butyrate and isoamyl acetate (Sigma-Aldrich). Odor-evoked responses to either the CS+ (odor paired with shock) or the CS− (unpaired odor) were imaged before and after conditioning. Electric shocks were delivered by two copper plates straddling the abdomen and the legs of the flies. Current was generated by a stimulator (Grass Technologies), with timing controlled by a microcontroller (Arduino). During conditioning, the CS+ was presented for 30 s and paired with six electric shocks (90 V) of 1.25-s duration each, with a 3.75-s interval. The first electric shock was delivered 5 s after the onset of the odor stimulation. After a 30-s rest interval, the CS− was presented for 30 s. Mushroom body regions were imaged and odor responses were analyzed as above. At the end of the experiment, each fly was shocked while imaging the MB to confirm effective shock delivery (12). Any flies that did not show clear Ca^{2+} responses to shocks were discarded from the analysis. For behavioral conditioning,

238Y-Gal4>UAS-bPAC flies and genetic controls were raised in complete darkness to avoid light-induced bPAC activation. Flies were trained and tested following a standard short-term memory protocol in dim red light as previously described (15). Briefly, groups of ~50 flies were exposed to an odor for 1 min (the CS+), paired with 12 90-V electric shocks. After a 30-s delay, a second odor was presented (the CS−). Flies were immediately transferred to a T maze and the performance index was calculated. Ethyl butyrate and isoamyl acetate were presented as the CS+ and CS− in a reciprocal paradigm.

Appetitive Conditioning. Appetitive conditioning was performed by pairing one odor (CS+) with sucrose reward, while a second odor (CS−) was unrewarded. During conditioning, the CS+ was presented for 30 s, and the flies were given simultaneous proboscis access to a 1 M sucrose solution. After a 30-s rest interval, the CS− was presented for 30 s. Odor-evoked responses to either the CS+ or CS− were imaged before and after conditioning. While imaging odor responses, the proboscis was immobilized with a loop of thin metal wire (A-M Systems) attached to a custom-built motorized micromanipulator. Flies were starved 18 to 24 h before the experiment. To feed the flies, the proboscis was released and the sucrose solution was presented through a metal pipette connected to a syringe pump controlled by a microcontroller (Arduino). Flies were monitored using a digital microscope (Vividia). The sucrose solution was supplemented with blue food coloring to confirm ingestion. Flies that did not show the presence of the blue dye in their abdomen were discarded from the analysis. In control experiments, odors were presented but the flies did not receive any sucrose reward.

Statistical Analysis. Analyses were performed using Prism (GraphPad) and Matlab (MathWorks). Normality was assessed with the D'Agostino and Pearson omnibus test. Two-sample comparisons were made with the Student's *t* test (parametric) or Mann–Whitney test (nonparametric). One-way hypotheses were tested with ANOVA, followed by Tukey's post hoc tests (parametric). Two-way hypotheses were tested by two-way ANOVA, followed by Sidak's multiple comparisons tests. Slopes and elevations of linear regression lines were compared with modified *t* tests (16). Categorical data were compared with χ^2 tests. Box plots represent the median with a line, first to third interquartile range with a box, and 10th to 90th percentiles with whiskers.

1. Jenett A, et al. (2012) A GAL4-driver line resource for *Drosophila* neurobiology. *Cell Rep* 2:991–1001.
2. Pfeiffer BD, et al. (2010) Refinement of tools for targeted gene expression in *Drosophila*. *Genetics* 186:735–755.
3. Aso Y, et al. (2014) The neuronal architecture of the mushroom body provides a logic for associative learning. *Elife* 3:e04577.
4. Séjourné J, et al. (2011) Mushroom body efferent neurons responsible for aversive olfactory memory retrieval in *Drosophila*. *Nat Neurosci* 14:903–910.
5. Boto T, Louis T, Jindachomthong K, Jalink K, Tomchik SM (2014) Dopaminergic modulation of cAMP drives nonlinear plasticity across the *Drosophila* mushroom body lobes. *Curr Biol* 24:822–831.
6. Shafer OT, et al. (2008) Widespread receptivity to neuropeptide PDF throughout the neuronal circadian clock network of *Drosophila* revealed by real-time cyclic AMP imaging. *Neuron* 58:223–237.
7. Zhao Y, et al. (2011) An expanded palette of genetically encoded Ca^{2+} indicators. *Science* 333:1888–1891.
8. Stierl M, et al. (2011) Light modulation of cellular cAMP by a small bacterial photoactivated adenylyl cyclase, bPAC, of the soil bacterium *Beggiatoa*. *J Biol Chem* 286:1181–1188.
9. Akerboom J, et al. (2013) Genetically encoded calcium indicators for multi-color neural activity imaging and combination with optogenetics. *Front Mol Neurosci* 6:2.
10. Fosque BF, et al. (2015) Labeling of active neural circuits in vivo with designed calcium integrators. *Science* 347:755–760.
11. Schindelin J, et al. (2012) Fiji: An open-source platform for biological-image analysis. *Nat Methods* 9:676–682.
12. Yu D, Akalal DB, Davis RL (2006) *Drosophila* alpha/beta mushroom body neurons form a branch-specific, long-term cellular memory trace after spaced olfactory conditioning. *Neuron* 52:845–855.
13. Yu D, Keene AC, Srivatsan A, Waddell S, Davis RL (2005) *Drosophila* DPM neurons form a delayed and branch-specific memory trace after olfactory classical conditioning. *Cell* 123:945–957.
14. Yu D, Ponomarev A, Davis RL (2004) Altered representation of the spatial code for odors after olfactory classical conditioning: Memory trace formation by synaptic recruitment. *Neuron* 42:437–449.
15. Tomchik SM, Davis RL (2009) Dynamics of learning-related cAMP signaling and stimulus integration in the *Drosophila* olfactory pathway. *Neuron* 64:510–521.
16. Zar JH (2010) *Biostatistical Analysis* (Pearson, Upper Saddle River, NJ), 5th Ed.

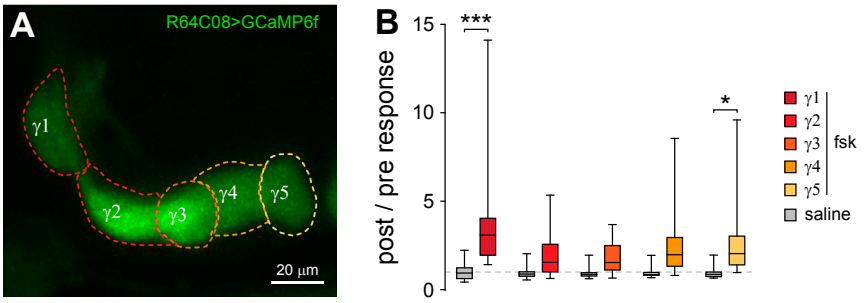

Fig. S1. Forskolin (fsk) increased responses across multiple subdomains of the mushroom body γ-lobe. Each compartment (γ1 to γ5) was analyzed with a separate region of interest (*A*), and controls were compared with forskolin-treated animals (*B*). There was a significant effect of forskolin treatment ($P < 0.001$; two-way ANOVA). Pairwise comparisons revealed significant differences in the γ1- and γ5-regions, though there was a trend in the same direction in all compartments ($n > 12$ per group). *$P < 0.05$, ***$P < 0.001$ (Sidak).

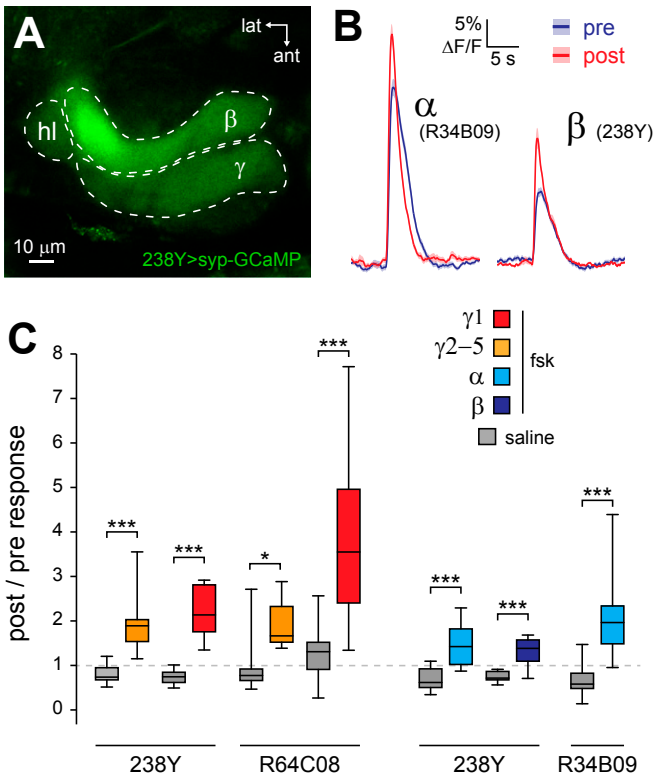

Fig. S2. Presynaptically tethered GCaMP revealed cAMP-dependent plasticity distributed across the MB γ- and α/β-lobes [heel, (hl)]. (*A*) Confocal image of syp-GCaMP3 in the MB β- and γ-lobes, driven with the broad MB driver 238Y-gal4. (*B*) Pre vs. post cAMP-elevation Ca^{2+} responses in the α-lobe (R34B09) and β-lobe (238Y). (*C*) Change in odor-evoked responses following pairing of odor with forskolin or saline across drivers and regions, imaged with syp-GCaMP3 ($n > 8$ per group). The γ-neurons were imaged using 238Y and R64C08, while α/β-neurons were imaged with 238Y and R34B09. *$P < 0.05$, ***$P < 0.001$ (Sidak).

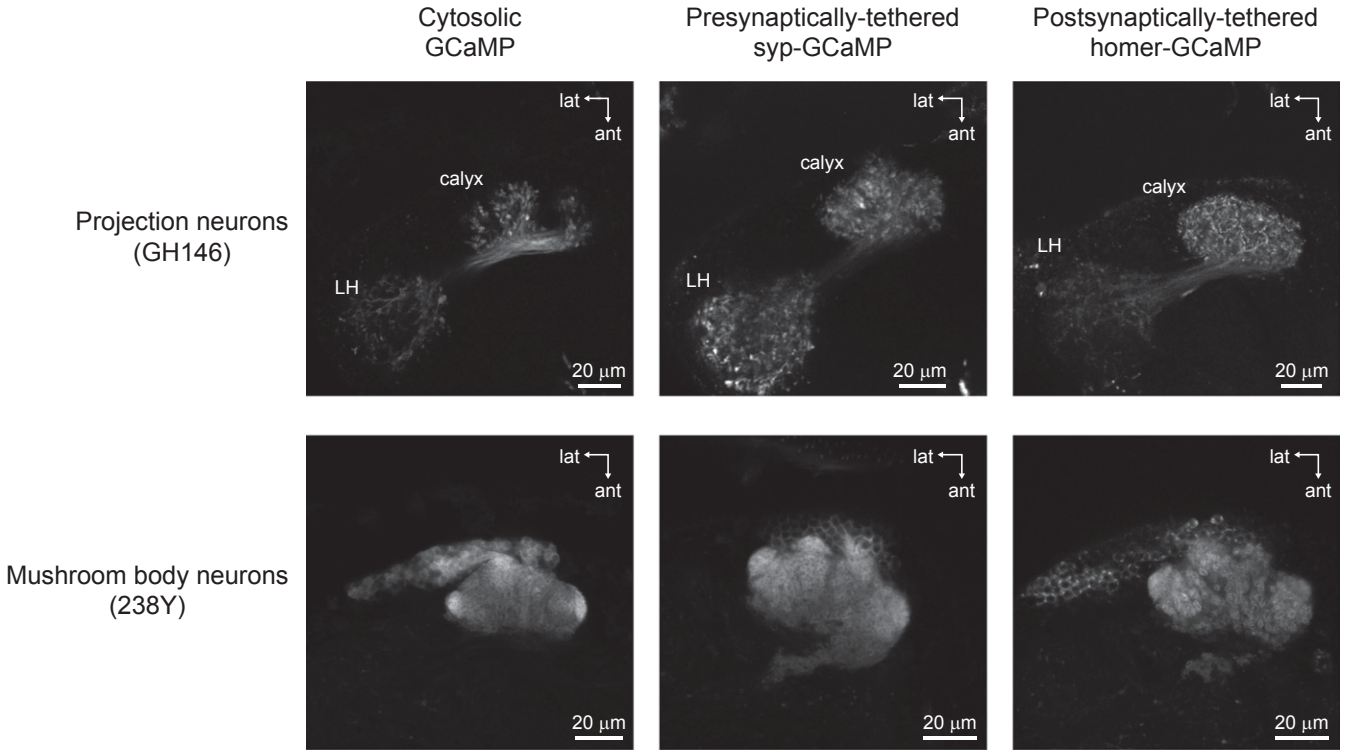

Fig. S3. Expression of GCaMP variants in the projection neurons (*Top*) and mushroom body neurons (*Bottom*). Images from projection neurons show the terminals in both the lateral horn (LH) and mushroom body calyx. Images of mushroom body neurons are zoomed in on the calyx. All three GCaMP variants, cytosolic uas-GCaMP6f, presynaptically tethered uas-syp-GCaMP3, and postsynaptically tethered uas-homer-GCaMP3, were expressed in each cell type. Fluorescence was imaged in the calyx, where projection neurons synapse with mushroom body neurons. Both cell types contain pre- and postsynaptic elements. Fluorescence is pseudocolored in white for maximum contrast.

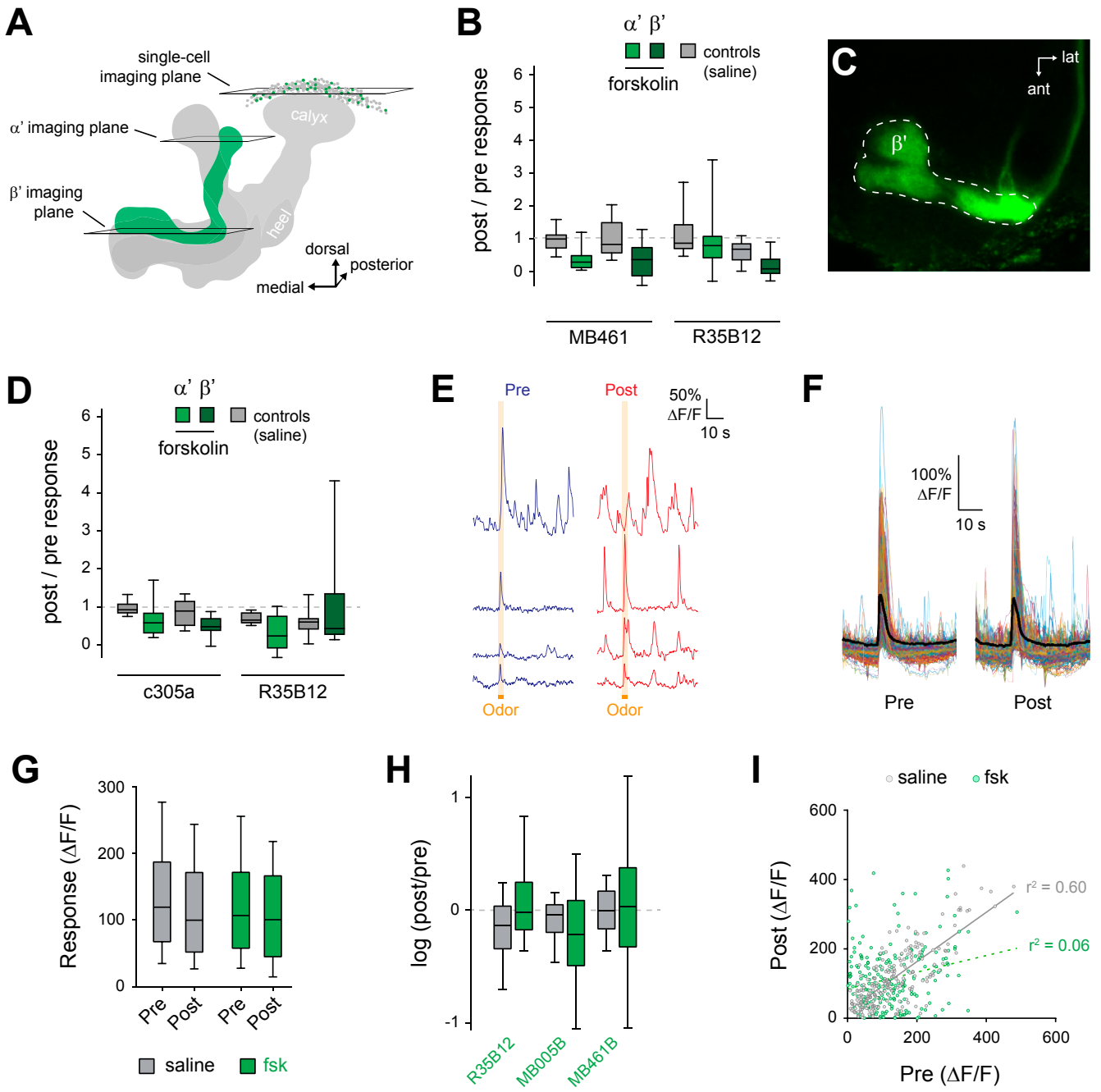

Fig. S4. Cyclic-AMP elevation increased spontaneous activity and affected odor-evoked activity heterogeneously in α′/β′-neurons. (*A*) Drawing of a frontal view of the MB, with the lobes and somata of α′/β′ highlighted in green. The approximate plane of section for imaging MB somata is indicated with a box. (*B*) Cytosolic GCaMP revealed no net change in odor-evoked Ca^{2+} transients in α′/β′-neurons following cAMP elevation with forskolin (MB461 $n = 12$ per group; R35B12 $n = 12$ or 13). The tips of the α′-lobe (α′3) and β′ were imaged in different flies. (*C*) Horizontal confocal section of the β′-lobe, expressing GCaMP6f under control of the α′/β′-selective R35B12-Gal4 driver. (*D*) Presynaptically tethered syp-GCaMP revealed no net change in odor-evoked Ca^{2+} transients in α′/β′-neurons following cAMP elevation with forskolin (c305a $n = 12$; R35B12 $n = 8$ to 10). (*E*) Time series traces showing the responses of four neurons before and after elevation of cAMP with forskolin. Following cAMP elevation, the neurons exhibited ongoing activity visible outside the odor delivery window. (*F*) Time series traces showing the responses of individual MB α′/β′-neurons pre and post cAMP elevation. Traces are pooled among α′/β′-selective drivers. (*G*) Magnitude of single-neuron, odor-evoked Ca^{2+} responses, pre and post forskolin application in MB α′/β′-neurons (pooled from all α′/β′-selective drivers). There was no main effect of treatment ($P = 0.14$; two-way ANOVA), but there was a significant effect of stimulus (pre vs. post) ($P = 0.016$). Pairwise comparisons did not reveal differences between pre vs. post responses in either saline- or forskolin-treated groups ($P > 0.05$; Sidak). (*H*) Change in odor-evoked Ca^{2+} responses among α′/β′-neurons, graphed as the ratio of post/pre treatment (forskolin vs. saline controls). Individual neurons were imaged in animals expressing GCaMP in one of three gal4 (or split-gal4) drivers: R35B12 (saline $n = 64$ neurons; forskolin $n = 65$), MB005B (saline $n = 83$; forskolin $n = 83$), or MB461B (saline $n = 70$; forskolin $n = 69$). Two-way statistical comparisons were not run due to high heteroscedasticity. (*I*) Post- vs. pretreatment Ca^{2+} responses. Linear regression lines are plotted for each group, with the forskolin regression line dashed due to the low r^2 value.

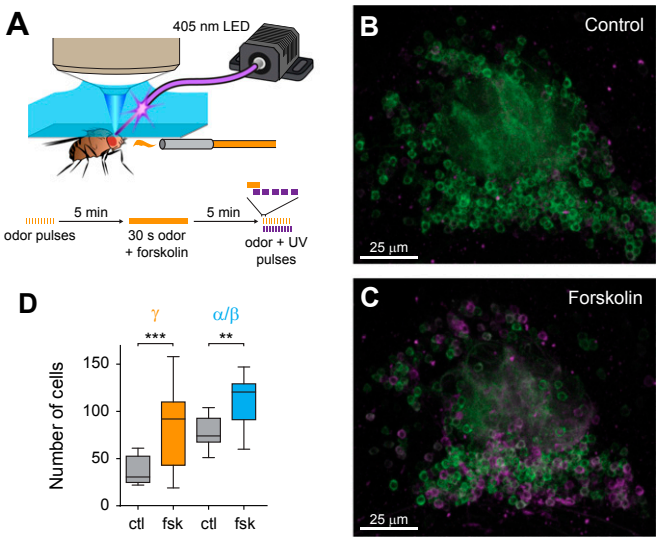

Fig. S5. Conditional activity labeling with CaMPARI reveals differential cAMP-dependent enhancement of responses in MB γ-neurons. (*A*) Diagram of the experimental apparatus and protocol. Flies were prepared for confocal imaging, and odor delivery was controlled as in Fig. 1*A*. A fiber-coupled LED was aimed into the head capsule to deliver 405-nm light pulses to the brain. Odor pulses were presented before and after pairing the odor with forskolin or saline (controls). The odor pulses were then paired with 405-nm light to photoconvert CaMPARI in neurons that were strongly activated by the odor. (*B*) Image of CaMPARI-expressing MB γ-neurons in a control (no forskolin) animal (1471-Gal4). (*C*) Image of CaMPARI-expressing MB γ-neurons in an animal in which cAMP was elevated with forskolin (1471-Gal4). (*D*) Quantification of the number of photoconverted neurons in the MB. CaMPARI was driven in the γ-neurons with the 1471 driver (saline $n = 10$; forskolin $n = 11$), or in α/β-neurons with the c739 driver (saline $n = 12$; forskolin $n = 12$). ctl, saline control. $^{**}P < 0.01$, $^{***}P < 0.001$ (Sidak).

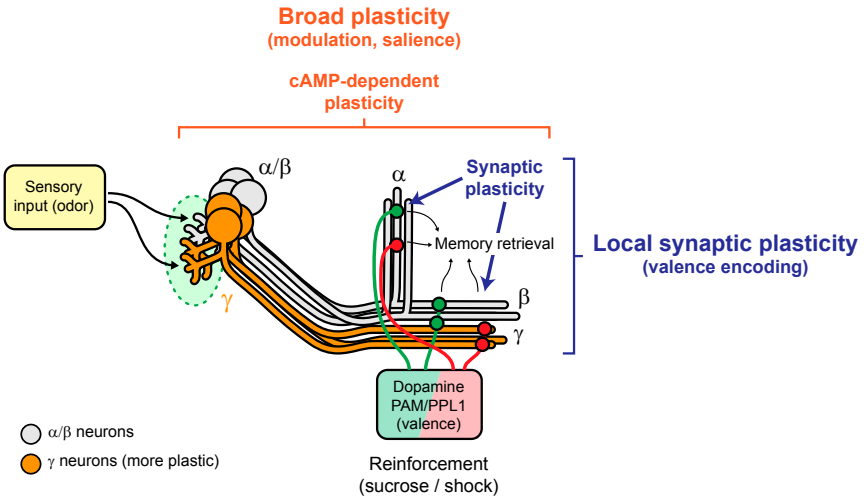

Fig. S6. Model of cAMP-dependent plasticity in the mushroom body. We propose that cAMP modulates olfactory responses of mushroom body neurons in two ways. First, cAMP-dependent plasticity affects responses of intrinsic mushroom body neurons in a cell type-specific manner, with γ-neurons differentially facilitated. This plasticity is observed across multiple spatial subdomains of mushroom body neurons, ultimately affecting multiple output neurons of opposing valence. Behaviorally, plasticity is generated following appetitive conditioning, and modulates responses to odors in a salience-dependent manner. Layered on top of this effect is localized synaptic plasticity that is driven by valence-specific dopaminergic neurons, and which drives behavioral approach/avoidance behavior by altering the flow of olfactory information to valence-specific output circuits. This form of plasticity may occur in either/both the pre- and post-synaptic side of the synapse between mushroom body neurons and the mushroom body output neurons.